

Impact of Parameters Variability on the Level of Human Exposure Due to Inductive Power Transfer

*Original*

Impact of Parameters Variability on the Level of Human Exposure Due to Inductive Power Transfer / Lagouanelle, P; Bottauscio, O; Pichon, L; Zucca, M. - In: IEEE TRANSACTIONS ON MAGNETICS. - ISSN 0018-9464. - STAMPA. - 57:6(2021), pp. 1-4. [10.1109/TMAG.2021.3062702]

*Availability:*

This version is available at: 11583/2974806 since: 2023-01-19T15:35:58Z

*Publisher:*

IEEE-INST ELECTRICAL ELECTRONICS ENGINEERS INC

*Published*

DOI:10.1109/TMAG.2021.3062702

*Terms of use:*

This article is made available under terms and conditions as specified in the corresponding bibliographic description in the repository

*Publisher copyright*

(Article begins on next page)

# Impact of Parameters Variability on the Level of Human Exposure Due to Inductive Power Transfer

Paul Lagouanelle<sup>1,2,3</sup>, Oriano Bottauscio<sup>4</sup>, Lionel Pichon<sup>1,2</sup>, and Mauro Zucca<sup>4</sup>

<sup>1</sup>Group of Electrical Engineering-Paris, CNRS, CentraleSupélec, Université Paris-Saclay, Gif-sur-Yvette, France

<sup>2</sup>Group of Electrical Engineering-Paris, CNRS, Sorbonne Université, Paris, France

<sup>3</sup>Dipartimento Energia, Politecnico di Torino, 10129 Turin, Italy

<sup>4</sup>Istituto Nazionale di Ricerca Metrologica (INRiM), 10135 Turin, Italy

**This article shows the effectiveness of combining non-intrusive stochastic techniques with 3-D modeling tools to build adequate surrogate models for the evaluation of human exposure close to a vehicle equipped with a wireless charging pad. A surrogate model is appropriate to deal with uncertainties and variabilities of parameters defining the electromagnetic problem. Numerical results obtained in the case of a light passenger vehicle illustrate the proposed methodology.**

**Index Terms**—Human exposure, inductive power transfer (IPT), stochastic methods.

## I. INTRODUCTION

**I**NDUCTIVE power transfer (IPT) is a key factor in the growth of electric mobility [1]. However, the large gap between transmitter and receiver implies a high level of stray field in the vicinity of the coils that, despite the presence of ferrite concentrators and aluminum shield, may represent a problem in terms of exposure to magnetic fields for passengers or bystanders during the charging operations. It is, therefore, needed to evaluate the level of exposure in order to be compliant with the relevant standards and guidelines for human exposure when designing a new IPT system.

In order to assess human exposure near IPT systems in automotive applications, adequate modeling methodologies have to be developed. The use of powerful 3-D models involving the wireless power transfer (WPT) system and the car-body produced reliable results at heavy computational cost for the radiated field around the system or induced in the human body [2], [3] and more recently on the magnetic field produced by Society of Automotive Engineers (SAE) J2954 coils [4]–[6]. The level of exposure is highly dependent on various physical and geometrical parameters: magnitude and phase of the currents in the coils, geometrical characteristics of the system, materials properties, possible misalignment and distance between transmitter and receiver, position of the human body, and so forth. Moreover, when building the real system, every parameter (physical or geometrical) might come with some given uncertainty, which also needs to be taken into account. Therefore, in order to fully predict the behavior of the IPT system for human exposure, one cannot simply use 3-D solvers.

Thus, by using stochastic tools with a given set of inputs and their corresponding outputs, one can build a metamodel

that interpolates the real model given by the 3-D solver. This resulting metamodel is a mathematical function that can be used easily to predict the outputs of the real model outside of the training data set. Therefore, it can be used to perform various analyses, such as the Sobol index sensitivity analysis [7] at a low computation cost. This allows dealing with the variability of all the parameters describing the electromagnetic problem. Such tools have already been used successfully in the past for the determination of specific rate absorption (SAR) in biological tissues due to mobile phones at microwave frequencies [8], [9]. The same goes for an automotive WPT system in the case of a simplified 3-D model, where the polynomial chaos and Kriging methods have been really efficient [10].

The objective of this article is to show the effectiveness of non-intrusive methods based on a combination of polynomial chaos expansions with Kriging in the case of a realistic passenger vehicle in assessing the sensitivity of the electromagnetic problem to several parameters. INRiM provided a 3-D finite element method (FEM) model of an electric vehicle charging station (EVCS) that includes a car-body of an S80 sedan car kindly provided by Volvo car company in the framework of the project [11]. The FEM model has been solved by varying the physical parameters of the metal car body and charging pad. The GeePs used the various results to develop accurate metamodels using the UQLab framework [12] to perform decent sensitivity analysis using Sobol indices.

## II. REALISTIC MODEL

### A. Charging Station Model

The studied EVCS has been modeled in the framework of the MICEV project [11], and it is considered with a central position for the IPT system (see Fig. 1). The 3-D finite element mesh has been built by means of the OPERA 3-D simulation software by Dassault Systèmes. The system has been limited to the car-chassis and the charging pad, whose rated power is up to 7.5 kW and the resonance frequency is 85 kHz. The current in the two coils was taken as sinusoidal, with the current in the receiving coil being the same amplitude as

Manuscript received November 3, 2020; revised January 31, 2021 and February 16, 2021; accepted February 19, 2021. Date of publication February 26, 2021; date of current version May 17, 2021. Corresponding author: P. Lagouanelle (e-mail: paul.lagouanelle@geeps.centralesupelec.fr).

Color versions of one or more figures in this article are available at <https://doi.org/10.1109/TMAG.2021.3062702>.

Digital Object Identifier 10.1109/TMAG.2021.3062702

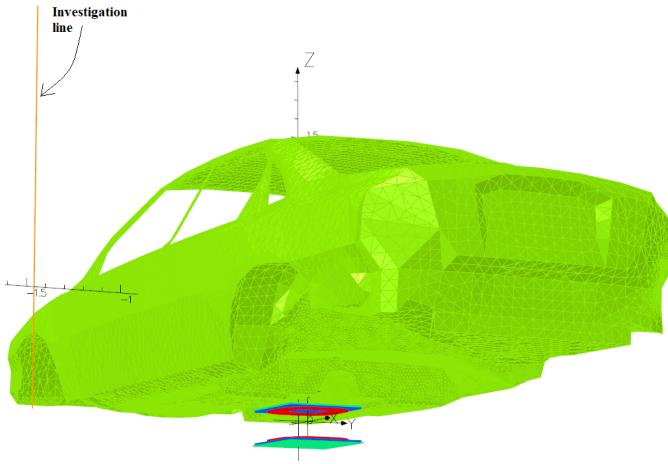


Fig. 1. 3-D FEM model mesh of the chassis: the positions of the charging pad and the investigation line.

that in the transmitting coil, i.e., 26 A peak. Being eight the turns, the total magnetomotive force in the coils is 208 A peak, but the electric current in the receiving coil had a 90° phase lag. The distance between the coils was 150 mm. The metal thickness of the chassis is assumed to be 1 mm. Due to the important skin effect, a surface impedance boundary condition (SIBC) is used Cirimele *et al.* [13].

The following input parameters have been considered for performing sensitivity analysis on our vehicle:

- 1) the conductivity of the chassis  $\sigma$ ;
- 2) the relative permeability of the chassis  $\mu_r$ ;
- 3) the relative permeability of the ferrite in the charging pad  $\mu_f$ ;
- 4) the radial misalignment between the center of the two coils  $\Delta x$  along the  $x$ -axis (axis of motion);
- 5) the radial misalignment between the center of the two coils  $\Delta y$  along the  $y$ -axis;
- 6) the gap between the two coils  $\Delta z$  along the  $z$ -axis (vertical axis).

The output ( $B$  hereafter) of our model is the amplitude of the magnetic flux density evaluated along a vertical line (101 points), which embodies a bystander position.

- 1)  $x = 0$  m.
- 2)  $y = -1.5$  m.
- 3) 101 values for  $z$  uniformly distributed from 0 to 2 m.

With such a system, the built-in mesh has around  $6 \cdot 10^6$  elements along with around  $7.7 \cdot 10^6$  edges. Thus, computing the model for a given set of input parameters is taking about 16 h (CPU time).

### B. Polynomial-Chaos-Kriging Metamodeling

Kriging is a stochastic interpolation algorithm that interpolates the local variations of the output  $\mathbf{B}$  as a function of the neighboring experimental design points, whereas the polynomial-chaos expansion approximates well the global behavior of  $\mathbf{B}$ . By combining the global and local approximation, a more accurate stochastic process can be achieved. Polynomial-chaos-Kriging (PCK) is defined as a universal

Kriging model, the trend of which consists of a set of orthonormal polynomials. Given an input  $X$  of the parameters, the output  $B(X)$  can be estimated by

$$\widehat{B}(X) = \sum_{\alpha \in \mathcal{A}} y_{\alpha} \psi_{\alpha}(X) + \sigma^2 Z(X, \omega) \quad (1)$$

where  $\sum_{\alpha \in \mathcal{A}} y_{\alpha} \psi_{\alpha}(X)$  is a weighted sum of orthonormal polynomials describing the trend of the PCK model, and  $\sigma^2$  and  $Z(X, \omega)$  denote the variance and the zero mean of the unit variance and stationary Gaussian process, respectively. Hence, PCK can be interpreted as a universal Kriging model with a specific trend.

1) *Consistency of the Metamodel:* Let us consider a set  $\{(X_1, B_1), \dots, (X_n, B_n)\}$  of  $n$  datapoints: a given set of input and their corresponding outputs. Using this set, one can build a metamodel  $\widehat{B}(X)$  with PCK. The accuracy of the metamodel is calculated using the mean leave-one-out error (LOO)

$$\text{LOO} = \frac{1}{n} \sum_{i=1}^n \left( \frac{\widehat{B}_{/i}(X_i) - B_i}{B_i} \right)^2 \quad (2)$$

where  $\widehat{B}_{/i}$  is the mean predictor that was trained using all  $(X, Y)$  but  $(X_i, B_i)$ . The LOO enables us to evaluate the consistency of the metamodel considering its build. If the LOO is close to 1, the metamodel is highly modified if one datapoint is missing, whereas the smallest it is, the least it will be modified.

2) *Accuracy of the Metamodel:* If one were to build a metamodel  $\widehat{B}_k(X)$  using a subset of  $k$  datapoints out of the aforementioned  $n$  datapoints, the accuracy of the predictor on the  $(n-k)$  remaining points  $\{(X_1, B_1), \dots, (X_{n-k}, B_{n-k})\}$  can be calculated using the out-of-sample-error (OSE)

$$\text{OSE} = \frac{1}{n-k} \sum_{i=1}^{n-k} \left( \frac{\widehat{B}_k(X_i) - B_i}{B_i} \right)^2. \quad (3)$$

The analysis of the OSE emphasizes something different than the LOO analysis does: if the OSE for  $k$  datapoints is extremely small, it means that, at the non-sampled points, there is almost no difference between the predictor and the real value. Hence, if the OSE for  $k$  datapoints is small enough, there was no need to compute  $n$  datapoints, but  $k$  is enough.

## III. NUMERICAL RESULTS AND DISCUSSION

PCK metamodeling has been used on several numerical results of our 3-D model in order to predict its behavior. Out of the available set of datapoints, only a part has been taken to build the metamodels in order to observe if the output model accuracy would be the same using all points or fewer.

### A. First Sweep: Three Input Parameters, $n = 24$ Datapoints

The first metamodels developed used an existing pre-computing data set (see Table I) regarding the three input parameters:  $X = (\sigma, \mu_r, \mu_f)$ .

Four different metamodels have been computed: one with the full set of  $n = 24$  datapoints; then, three metamodels calculated by randomly taking  $k = 18, 12,$  and  $6$  datapoints out of the full set. The goal was to observe using the OSE

TABLE I  
OUR FIRST DATA SET ( $n = 24$ )

$\mu_r$	$\sigma$ ( $\text{S m}^{-1}$ )	$\mu_f$	$\mu_r$	$\sigma$ ( $\text{S m}^{-1}$ )	$\mu_f$
1	0	2000	300	0	100
1	$10^6$	2000	300	0	200
1	$5 \cdot 10^6$	2000	300	0	500
1	$10^7$	2000	300	0	1000
100	0	2000	300	0	2000
100	$10^6$	2000	300	$10^6$	2000
100	$5 \cdot 10^6$	2000	300	$2 \cdot 10^6$	100
100	$10^7$	2000	300	$2 \cdot 10^6$	200
200	0	2000	300	$2 \cdot 10^6$	500
200	$10^6$	2000	300	$2 \cdot 10^6$	1000
200	$5 \cdot 10^6$	2000	300	$5 \cdot 10^6$	2000
200	$10^7$	2000	300	$10^7$	2000

TABLE II  
LOO, OSE, AND SOBOLEW SENSITIVITY ANALYSIS  
FOR OUR FIRST METAMODELS

Subset size ( $k$ samples)	LOO	OSE	$S_{\mu_r}$	$S_{\sigma}$	$S_{\mu_f}$
24	$2.29 \cdot 10^{-3}$	NaN	0	0.842	$4.34 \cdot 10^{-3}$
18	$1.97 \cdot 10^{-3}$	$6.50 \cdot 10^{-4}$	0	0.918	0
12	$3.26 \cdot 10^{-2}$	$5.67 \cdot 10^{-2}$	0	0.941	0
6	0.180	1.78	0	0.609	0

if initially computing less than 24 points would have still produced an accurate metamodel on the given domain. The results are displayed in Table II.

The first noticeable thing is the LOO, which is even better with  $k = 18$  instead of 24 datapoints, meaning that the metamodel produced with less randomly chosen points is more consistent with itself. Moreover, the LOO for  $k = 12$  samples is still good (less than 4%), and the OSE is also less than 6%; thus, a metamodel with half the points could almost have been enough for the considered parameters domain. Unfortunately, six points are not enough to produce an accurate and consistent metamodel and perform a sensitivity analysis on our model. The significant parameter by far here is the conductivity of the frame, while both relative permeabilities have almost no influence on the output  $B$  vector for this data set. When plotting the  $B$ -field values against the distance for one of the six datapoints remaining when building the  $k = 18$  datapoints metamodel (see Fig. 2), it can be observed that the metamodel can perfectly interpolate the input model to produce an estimate accurate enough to perform sensitivity analysis that could help designing a WPT system compliant to the safety guidelines.

Thus, this first attempt at metamodeling our WPT system is promising but, when looking at the data set, especially its distribution in the parameter space (see Fig. 3), it can be seen that the sample distribution is highly nonuniform. By building a metamodel with fewer randomly chosen datapoints out of the given data set, some area of the parameter space could be avoided, and therefore, a totally inaccurate metamodel would be computed. That is why, for the next attempt, we decided to compute a more uniformly distributed sweep on our WPT model.

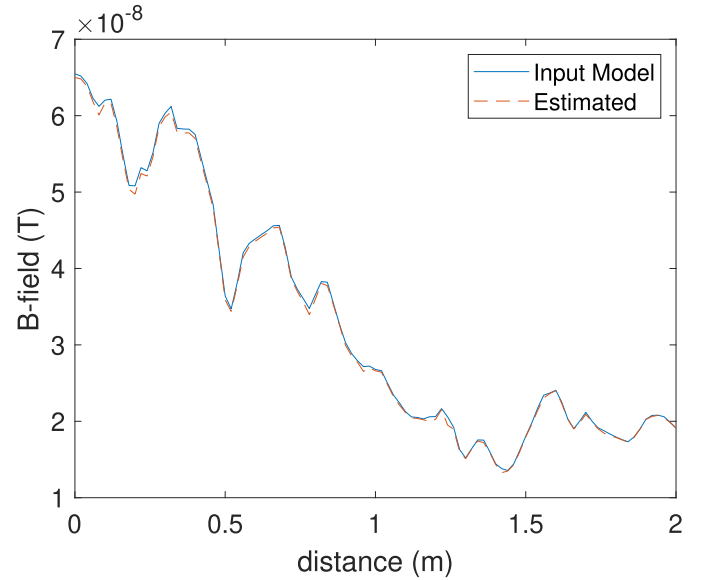


Fig. 2.  $B$ -field against the distance for the model with 18/24 datapoints (estimated) against the one with the full data set (input model) for a given datapoint ( $\mu_r = 200$ ,  $\mu_f = 2000$ , and  $\sigma = 5 \cdot 10^6 \text{ S m}^{-1}$ ).

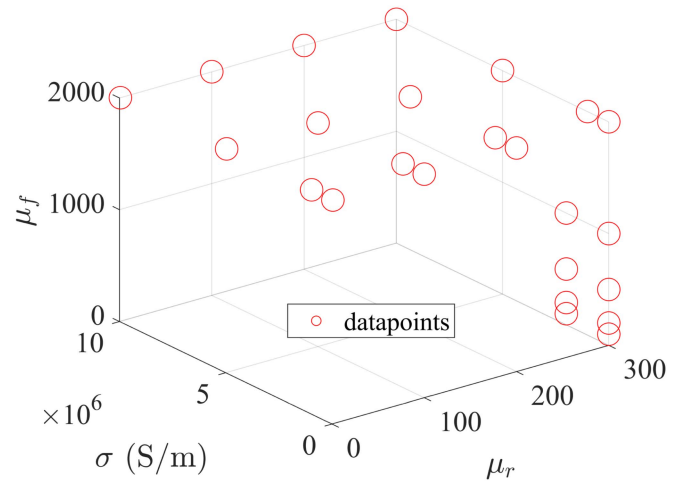


Fig. 3. Distribution of the different samples in the parameter space for our first data set ( $n = 24$ ).

### B. Second Sweep: Five Input Parameters, $n = 78$ Datapoints

For the second data set, the samples are uniformly distributed in the chosen parameter space.

$X = (\mu_r, \sigma, \Delta x, \Delta y, \Delta z)$ . The following sweep has been computed on our WPT model.

- 1)  $\sigma \in \{0, 10^6\} \text{ S m}^{-1}$ .
- 2)  $\mu_r \in \{1, 100, 300\}$ .
- 3)  $\Delta x \in \{-75, 75\} \text{ mm}$ .
- 4)  $\Delta y \in \{-100, 0, 100\} \text{ mm}$ .
- 5)  $\Delta z \in \{-50, 0, 50\} \text{ mm}$ .

The same analysis as previous has been performed on this data set of  $n = 78$  points resulting in the LOO, OSE, and sensitivity analysis displayed in Table III.

These new metamodels are all consistent: indeed, there is less than 5% of LOO even when sampling only a quarter ( $k =$

TABLE III  
LOO, OSE, AND SOBEL SENSITIVITY ANALYSIS  
FOR OUR SECOND METAMODELS

Subset size ( $k$ samples)	LOO	OSE	$S_{\mu_r}$
78	$2.76 \cdot 10^{-4}$	NaN	$1.79 \cdot 10^{-3}$
58	$1.11 \cdot 10^{-3}$	$4.62 \cdot 10^{-4}$	$1.67 \cdot 10^{-3}$
39	$1.53 \cdot 10^{-2}$	$5.61 \cdot 10^{-3}$	$2.45 \cdot 10^{-3}$
19	$4.02 \cdot 10^{-2}$	0.248	$2.28 \cdot 10^{-3}$
$S_\sigma$	$S_{\Delta x}$	$S_{\Delta y}$	$S_{\Delta z}$
0.690	$2.09 \cdot 10^{-4}$	$9.67 \cdot 10^{-2}$	0.123
0.656	$2.55 \cdot 10^{-3}$	0.120	0.141
0.581	$1.72 \cdot 10^{-4}$	0.127	0.231
0.584	$4.43 \cdot 10^{-4}$	$9.70 \cdot 10^{-2}$	0.253

19) of the data set. However, for this metamodel, the OSE is too high ( $> 20\%$ ); thus, it cannot be used as an accurate predictor for the WPT system. The predictor with half the points ( $k = 39$ ) is even more accurate (OSE  $\simeq 6\%$ ) than the one from the first set. Using a more uniform parameter space enabled us to build a more consistent and more accurate metamodel with fewer points.

Even with more parameters as the previous analysis, the metamodels computed on this sweep allowed an equally accurate sensitivity analysis with the car-body conductivity still being the significant parameter against new geometrical parameters. The Sobol indices of the five parameters are here really useful for future computations. First, the influence of the relative permeability and the coils misalignment along the axis of motion is negligible against the misalignment along the  $y$ -axis and the  $z$ -axis and the car-body lamination conductivity. Thus, the future sensitivity analysis on these five parameters can be reduced to three parameters, or fewer samples can be taken from the non-significant parameters, and more samples can be given to the significant ones. Then, such an analysis can help with the design of real WPT systems where greater care should be given to the uncertainties on dimensioning the chassis conductivity and the system along the  $y$ - and  $z$ -axes.

#### IV. CONCLUSION

The stray magnetic field on a bystander position has been obtained using a PCK metamodel in a modeled realistic EVCS. PCK metamodels enabled us to examine the effects of different physical or geometrical parameters on the output field of our IPT system at a low computation cost. Less computed datapoints will be needed in the future in order to verify the compliance of the system with the guidelines for human exposure. The analysis presented in this article will

now be extended by using more realistic configurations: various possible positions around the car will be investigated, and a full voxelized model for the human body will be used.

#### ACKNOWLEDGMENT

The results presented here are developed in the framework of the 16ENG08 Metrology for Inductive Charging of Electric Vehicles (MICEV) Project and supported in part by the European Metrology Programme for Innovation and Research (EMPIR) cofinanced by the Participating States and in part by the European Union's Horizon 2020 Research and Innovation Program.

#### REFERENCES

- [1] V. Cirimele, M. Diana, F. Freschi, and M. Mitolo, "Inductive power transfer for automotive applications: State-of-the-art and future trends," *IEEE Trans. Ind. Appl.*, vol. 54, no. 5, pp. 4069–4079, Sep. 2018.
- [2] V. Cirimele, F. Freschi, L. Giaccone, L. Pichon, and M. Repetto, "Human exposure assessment in dynamic inductive power transfer for automotive applications," *IEEE Trans. Magn.*, vol. 53, no. 6, pp. 1–4, Jun. 2017.
- [3] M. Feliziani, S. Cruciani, T. Campi, and F. Maradei, "Near field shielding of a wireless power transfer (WPT) current coil," *Prog. Electromagn. Res. C*, vol. 77, pp. 39–48, 2017. [Online]. Available: <http://www.jpier.org/PIERC/pier.php?paper=17042804>, doi: [10.2528/PIERC17042804](https://doi.org/10.2528/PIERC17042804).
- [4] K. Miwa, T. Takenaka, and A. Hirata, "Electromagnetic dosimetry and compliance for wireless power transfer systems in vehicles," *IEEE Trans. Electromagn. Compat.*, vol. 61, no. 6, pp. 2024–2030, Dec. 2019.
- [5] I. Liorni *et al.*, "Assessment of exposure to electric vehicle inductive power transfer systems: Experimental measurements and numerical dosimetry," *Sustainability*, vol. 12, no. 11, p. 4573, Jun. 2020.
- [6] *Wireless Power Transfer for Light-Duty Plug-in/Electric Vehicles and Alignment Methodology*, Standard J2954, S. Standard, vol. 9, 2016, p. 2019.
- [7] I. M. Sobol, "Global sensitivity indices for nonlinear mathematical models and their Monte Carlo estimates," *Math. Comput. Simul.*, vol. 55, nos. 1–3, pp. 271–280, Feb. 2001.
- [8] D. Voyer, F. Musy, L. Nicolas, and R. Perrussel, "Probabilistic methods applied to 2D electromagnetic numerical dosimetry," *COMPEL-Int. J. Comput. Math. Electr. Electron. Eng.*, vol. 27, no. 3, pp. 651–667, May 2008.
- [9] J. Silly-Carette, D. Lautru, M.-F. Wong, A. Gati, J. Wiart, and V. F. Hanna, "Variability on the propagation of a plane wave using stochastic collocation methods in a bio electromagnetic application," *IEEE Microw. Wireless Compon. Lett.*, vol. 19, no. 4, pp. 185–187, Apr. 2009.
- [10] P. Lagouanelle, V.-L. Krauth, and L. Pichon, "Uncertainty quantification in the assessment of human exposure near wireless power transfer systems in automotive applications," in *Proc. AEIT Int. Conf. Electr. Electron. Technol. Automot. (AEIT AUTOMOTIVE)*, Jul. 2019, pp. 1–5.
- [11] M. Zucca *et al.*, "Metrology for inductive charging of electric vehicles (MICEV)," in *Proc. AEIT Int. Conf. Electr. Electron. Technol. Automot. (AEIT AUTOMOTIVE)*, Jul. 2019, pp. 1–6.
- [12] S. Marelli and B. Sudret, "UQLab: A framework for uncertainty quantification in MATLAB," in *Proc. 2nd Int. Conf. Vulnerability Risk Anal. Manage. (ICVRAM)*. Liverpool, U.K.: Univ. of Liverpool, Jul. 2014, pp. 2554–2563, doi: [10.1061/9780784413609.257](https://doi.org/10.1061/9780784413609.257).
- [13] V. Cirimele, F. Freschi, L. Giaccone, and M. Repetto, "Finite formulation of surface impedance boundary conditions," *IEEE Trans. Magn.*, vol. 52, no. 3, pp. 1–4, Mar. 2016.